ICASSP 2021 - 2021 IEEE International Conference on Acoustics, Speech and Signal Processing (ICASSP) | 978-1-7281-7605-5/20/$31.00 ©2021 IEEE | DOI: 10.1109/ICASSP39728.2021.9413357

# HIDE CHOPIN IN THE MUSIC: EFFICIENT INFORMATION STEGANOGRAPHY VIA RANDOM SHUFFLING

*Zhun Sun[1], Chao Li[2], Qibin Zhao[2]*

*zhunsun@gmail.com, {chao.li, qibin.zhao}@riken.jp*
[1]Bigo Technology PTE. LTD, Singapore
[2]Center for Advanced Intelligence Project, RIEKN, Tokyo, Japan

**ABSTRACT**

Information steganography is a family of techniques that hide secret messages into a carrier; thus, the messages can only be extracted by receivers with a correct key Although many approaches have been proposed to achieve this purpose, historically, it is a difficult problem to conceal a large amount of information without occasioning human perceptible changes. In this paper, we explore the room introduced by the low-rank property of natural signals (*i.e.*, images, audios), and propose a training-free model for efficient information steganography, which provides a capacity of hiding full-size images into carriers of the same spatial resolution. The key of our method is to *randomly shuffle* the secrets and carry out a simple reduction summation with the carrier. On the other hand, the secret images can be reconstructed by solving a convex optimization problem similar to the ordinary tensor decomposition. In the experimental analysis, we carry out two tasks: concealing a full-RGB-color image into a gray-scale image; concealing images into music signals. The results confirm the ability of our model to handle massive secret payloads. The code of our paper is provided in `https://github.com/minogame/icassp-SIC`.

***Index Terms*—** Image Steganography, Tensor Decomposition, Privacy Protection, Image Signal Processing

## 1. INTRODUCTION

Have you ever listened to a song and felt like the music was painting a picture in your mind, or sending you secret messages? Oddly enough, that might not have been your brain playing tricks on you. Actually, the information steganography technique plays an essential role in our daily life for copyright-ownership control, privacy protection, and covert communication [1, 2, 3].

Most of the existing steganography approaches are achieved by replacing or modifying least significant bits (LSB) with the secret information in spatial [4, 5, 6, 7, 8, 9, 10], or transform [11, 12, 13, 14, 15] domains. The basic motivation of these methods is to carefully manipulate the LSB for embedding messages, such that the resulted distortions would be statistically difficult to be distinguished. However, the payload capacity is upper bounded by the original LSB method, *i.e.* 1 or 2 bits can be utilized for each pixel [4], which is not satisfying when dealing with heavy payloads such as a whole image of the same resolution. Although several deep-learning-based methods are recently proposed to improve the efficiency of image concealing, the training procedure is hungry with the scale of the dataset. Furthermore, the bias between training and test data may decrease the performance in practice [16].

To solve the aforementioned problems, we propose a training-free model that can effectively conceal the images into various types of carriers (see Fig. 1 for example). In our model, we leverage a common algebraic property owned by various datasets, *i.e.* low-rankness, for information steganography. The low-rank structure is a global characteristic of the data, allowing it to be embedded onto a lower-dimensional subspace under a certain tolerated error, *i.e.* approximated by a low-rank matrix. Such low-rank structures do ubiquitously exist in various real-life datasets.

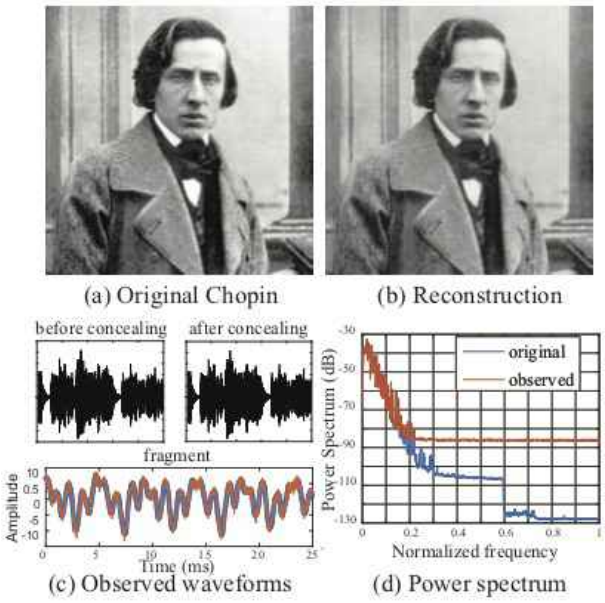


**Fig. 1**: Example of concealing a full-size secret image into a piece of music. Sub-figures (a) and (b) illustrate the original secret image and the corresponding reconstruction, respectively. Sub-figure (c) shows the waveform of the cover carrier, including the waveform before concealing (left-top), after concealing (right-top) and a fragment for comparison (bottom). Sub-figure (d) shows the power spectrum of the music signal before and after concealing. See Section 3.2 for the experimental setting and discussion.

Although former studies have considered the rooms provided by the low-rank structure [17, 18], they mainly multiply the singular values or vectors, and only a few bits can be hidden in these approaches. In contrast, inspired by the studies for the latent convex tensor decomposition (LCTD) [19], we consider the concealing and reconstruction as a matrix/tensor decomposition problem. We propose to replace the tensor unfolding operation in LCTD with the "randomly shuffling" operation. This approach not only provides the essential incoherence

for the decomposition model [20] but also increases the privacy security due to the randomness. The main contributions of our work can be summarized as follows: First, we propose a training-free model for image concealing, which leverages the low-rank structures of both carrier and secret images. Second, we experimentally demonstrate that the effectiveness and efficiency of the proposed model, in the case of heavy payload (*i.e.* hide a full-size RGB image into a grayscale image), and the case of cross-domain (*i.e.* hide an image into a snatch of music.)

## 2. PROPOSED METHOD

In this section, we describe the technical detail about the concealing and reconstruction scheme of the proposed method. We represent the *carrier* by a matrix $\mathbf{C} \in \mathbb{R}^{m\times n}$ and denote a set of $I$ secret images as the matrices $\mathbf{A}_i \in \mathbb{R}^{m\times n}$, $i \in [I]$, where $[I]$ denotes the set of integers from 1 to $I$. After concealing, we use the matrix $\mathbf{X}$ with the same size to represent the *observation*, which is perceptively similar to the carrier but contains the secret messages.

### 2.1. Concealing scheme

Before concealing, we define a random shuffling operation for each secret image. Roughly speaking, random shuffling for a given image means that we spatially rearrange pixels of that image to different locations.

In the concealing procedure, we first normalize each secret image by removing the mean value, dividing it by the standard deviation, and then conducting the random shuffling operations. We then sum all the shuffled secret images up to generate the "payload" in concealing. Next, we multiply the payload matrix by a scalar $\sigma$ to control the its strength for the trade-off between security and efficiency.

Mathematically, we represent the shuffling operations as a series of linear mappings $R_i : \mathbb{R}^{m\times n} \to \mathbb{R}^{m\times n}$. Thus the shuffled secrets are denoted by $R_i(\mathbf{A}_i)$, $\forall i$. Therefore, the concealing procedure can be formulated as[1]

$$\mathbf{X} = \underbrace{\mathbf{C}}_{carrier} + \underbrace{\sigma \sum_{i=1}^{I} R_i(\mathbf{A}_i)}_{payload}. \tag{1}$$

In practice, it is not necessary for the carrier to have a matrix form as $\mathbf{C}$. The carrier can have arbitrary forms such as vector (*e.g.*time series) and tensor (*e.g.*multi-way arrays). In our model, we can *reshape* the carrier into a matrix form. In the following sections, we demonstrate that any signal in its matrix form can be used as the carrier as long as its matrix form has a low-rank structure.

**Analysis of security.** It is worth mentioning that the spatial structures of the shuffled images would be completely destroyed due to the pixel-wise rearrange operations, and the correlation between the entries in the payload matrix would be weak due to the random choice of the shuffling operations. Therefore, based on the central limit theorem in probability theory, the pixels of the reduced payloads tend to be distributed normally and independently. Therefore, it implies the difficulty of distinguishing the statistical properties payloads from the additive white Gaussian noise (AWGN). Hence, the attackers cannot detect the secret messages easily by analyzing the statistical properties. Furthermore, reconstructing the secret images without the knowledge of the random shuffling operations is an NP-complete problem [21]. This leads to a more secure concealing system; even the carrier is fully exposed to the attackers.

[1]Here we ignore the normalization for brevity.

### 2.2. Reconstruction scheme

To extract the secret images, we solve the inverse problem of the image concealing. It implies that we need to reconstruct $\mathbf{A}_i$, $i \in [I]$ only with the observation $\mathbf{X}$ and the shuffling operations $R_i$'s. This inverse problem is obviously ill-posed because the number of unknowns is significantly more than the number of knowns. Inspired by the previous studies on matrix/tensor completion [22] and the robust principal component analysis (RPCA) [23], we solve this problem by further regulating the rank of both the carrier $\mathbf{C}$ and the secret images $\mathbf{A}_i, \forall i$. This allows us eliminating the ambiguity of the solution. Specifically, the secret images can be reconstructed by solving the following optimization problem:

$$\begin{aligned}\min_{\mathbf{C},\mathbf{A}_i,i\in[I]} &\|\mathbf{C}\|_* + \sum_{i=1}^{I} \|\mathbf{A}_i\|_* \\ &+ \frac{\lambda}{2}\left\|\mathbf{X} - \left(\mathbf{C} + \sigma\sum_{i=1}^{I} R_i(\mathbf{A}_i)\right)\right\|_F^2\end{aligned} \tag{2}$$

where $\|\cdot\|_*$ denotes the nuclear norm which equals the sum of the singular values of the matrix, $\|\cdot\|_F$ denotes the Frobenius norm, and $\lambda$ denotes the tuning parameter *w.r.t.* the strength of the noise. Due to the fact that the nuclear norm is the convex approximation of the matrix rank [24], minimizing the objective function in (2) is equivalent to looking for the low-rank solutions which satisfy the model (1). If both the carrier and the secret images obey the low-rank assumption, we can reconstruct the hidden secret images from the observation by solving (2).

To solve the optimization problem (2), we alternately update $\mathbf{C}$ and $\mathbf{A}_i$, $i \in [I]$ at each iteration. When updating the carrier $\mathbf{C}$, we treat $\mathbf{A}_i$, $\forall i$ as constants. Thus in this case the objective function of (2) can be rewritten as

$$f(\mathbf{C}) = \|\mathbf{C}\|_* + \frac{\lambda}{2}\left\|\left(\mathbf{X} - \sigma\sum_{i=1}^{I} R_i\left(\mathbf{A}_i\right)\right) - \mathbf{C}\right\|_F^2 + C_A, \tag{3}$$

where $C_A$ denotes the constant that contains the residual in (2). Note that minimizing (3) has a closed-form solution, which is given by

$$\mathbf{C}^+ := D_{\frac{1}{\lambda}}\left(\mathbf{X} - \sigma\sum_{i=1}^{I} R_i\left(\mathbf{A}_i\right)\right), \tag{4}$$

where $D_{\frac{1}{\lambda}}(\cdot)$ denotes the soft-thresholding operation [25]. If $\mathbf{X} = \mathbf{U}\mathbf{D}\mathbf{V}^\top$ is the singular value decomposition (SVD) of $\mathbf{X}$, then $\mathbf{D}_{\frac{1}{\lambda}}(\mathbf{X}) = \mathbf{U}\bar{\mathbf{D}}\mathbf{V}^\top$, where the entries $\bar{\mathbf{D}}(i,j), \forall i,j$ are defined to be

$$\bar{\mathbf{D}}(i,j) = \begin{cases} \mathbf{D}(i,j) - \frac{1}{\lambda} & \mathbf{D}(i,j) > \frac{1}{\lambda} \\ 0 & \text{otherwise} \end{cases}. \tag{5}$$

Likewise, we update the secret images $\mathbf{A}_i$ by the following equation:

$$\mathbf{A}_i^+ := D_{\frac{1}{\lambda}}\left(R_i^{-1}\left(\mathbf{X} - \mathbf{C} - \sigma\sum_{j\neq i}^{I} R_j\left(\mathbf{A}_j\right)\right)\right), \tag{6}$$

where $R_i^{-1}$ denotes the inverse operation of the random shuffling $R_i$. The theoretical analysis on the identifiability of the model can be seen in our previous work [26].

### 2.3. Tricks

Besides the main body of our model, we also employ additional 3 tricks to speed up the reconstruction procedures when improving the performance of the proposed algorithm.

**Table 1**: Performance comparison between the LSB and proposed methods. We split the datasets to two sub-sets, denote as **SET A** (carrier: Finger secret: DTD, Face) and **SET B** (carrier: X-ray secret: Live, Anime). PSNRs between the carrier and observation, and the clean and reconstructed secret, are given under "car./obv." and "scr./rec.", respectively.

| Method | SET A | | SET B | |
|---|---|---|---|---|
| | car./obv. | scr./rec. | car./obv. | scr./rec. |
| LSB(1bit) | 31.23 | 12.84 | 34.88 | 12.44 |
| LSB(2bits) | 14.99 | 20.52 | 18.61 | 20.44 |
| **SIC**$_{\sigma=0.05}$ | 27.60 | 21.44 | 29.79 | 21.90 |
| **SIC**$_{\sigma=0.10}$ | 22.65 | 21.87 | 24.87 | 22.92 |

#### *2.3.1. Initialization*

A good initialization significantly accelerates the convergence of the optimization. In the concealing procedure, we let the parameters $\sigma$ to be a small value to reduce the distortion on the carrier. Hence, for reconstruction, we expect that the main information of the secrets is contained in the several smallest singular values of the shuffled observations and their corresponding singular vectors. Inspired by such fact, we initialize the secret images through the SVD of the observation $\mathbf{X}$ under the corresponding inverse-shuffling operation. Specifically, for the $i$th secret images, we first use SVD to decompose the inverse-shuffled observation, *i.e.* $R_i^{-1}(\mathbf{X}) = \mathbf{U}_{\mathbf{X}}\mathbf{D}_{\mathbf{X}}\mathbf{V}_{\mathbf{X}}^{\top}$. Subsequently, we construct the initial value of $\mathbf{A}_i$ using $\mathbf{A}_i^{init} := \mathbf{U}_{\mathbf{X}}\tilde{\mathbf{D}}_{\mathbf{X}}\mathbf{V}_{\mathbf{X}}^{\top}$, where $\tilde{\mathbf{D}}_{\mathbf{X}}$ equals $\mathbf{D}_{\mathbf{X}}$ but only keeps the several smallest singular values. In the experiments, we set this number to be 5, which accelerates the convergence three times faster.

#### *2.3.2. Sketching*

From the updating rules (4) and (6) we see that the main computation cost comes from the SVD operations of the matrix. Assume both the carrier and secret images are the matrices of the size $n \times n$, then the computational complexity of the reconstruction equals $\mathcal{O}(In^3)$ at each iteration. In our experiments, we employ the sketching trick [27] for the acceleration of SVD. Specifically, to update the matrix $\mathbf{A}_i$ by (6), we need to calculate the SVD of $\mathbf{Y}_i := R_i^{-1}\left(\mathbf{X} - \mathbf{C} - \sigma\sum_{j\neq i}^{I} R_j\left(\mathbf{A}_j\right)\right)$. With the sketching trick, we first generate a Gaussian random projection matrix $\mathbf{P}_i \in \mathbb{R}^{n\times l}$, where $l$ is the dimension to be projected. Then we calculate the left singular vectors of the projected matrix $\mathbf{Y}_i\mathbf{P}_i$ using QR decomposition, *i.e.* $[\hat{\mathbf{U}}_i, \sim] = qr(\mathbf{Y}_i\mathbf{P}_i)$. After achieving the matrix $\hat{\mathbf{U}}_i$, we get the SVD of $\mathbf{Y}_i$ as $\mathbf{Y}_i = \hat{\mathbf{U}}_i\mathbf{D}_{tmp}\mathbf{V}_{tmp}^{\top}$, where $\hat{\mathbf{U}}_i^{\top}\mathbf{Y}_i = \mathbf{U}_{tmp}\mathbf{D}_{tmp}\mathbf{V}_{tmp}^{\top}$ is the SVD of $\hat{\mathbf{U}}_i^{\top}\mathbf{Y}_i$. With the sketching trick, the computational complexity can be theoretically reduced from $\mathcal{O}(In^3)$ to $\mathcal{O}(In^2)$ in each iteration if the dimension of the random projection is sufficiently small. On the other hand, the sketched SVD will result in unavoidable noise in the reconstructions. In the experiments, we choose the $l$ to be half of the dimension $n$ to balance the reconstruction speed and quality.

#### *2.3.3. Singular value truncation*

Since the reconstruction error is deterministically bounded by the rank of the data. Although in Equation 2 we approximate it with the nuclear norm, in practice, the non-zero small singular values could confound the extraction of secret pixels. Given the fact that these singular values do not affect the appearances of an image, we consider to pre-progress the carrier by $\mathbf{C} = \mathbf{U}_{\mathbf{c}}\hat{\mathbf{D}}_{\mathbf{c}}^{r}{\mathbf{V}_{\mathbf{c}}}^{T}$, where $\hat{\mathbf{D}}_{\mathbf{c}}^{r}$ indicates the $r$ smallest singular values are truncated from $\mathbf{D}_{\mathbf{c}}$. The influence of $r$ will be examined in Section 4.2.

## 3. REAL-WORLD DATA EXPERIMENTS

### 3.1. Concealing images into images

In this section, we compare the performance of the proposed method with baseline methods. To demonstrate the effectiveness and efficiency of our method, we carry out a task that is typically unachievable by the ordinary methods, that is, we conceal one full-size *RGB color* image into one *grayscale* image. We employ six datasets from different domains as the carriers and the secret images: the Describable Textures Dataset [28], Image Quality Assessment Database [29], MIT-CBCL face recognition database [30], Anime Illustration Dataset[2], Fingerprint recognition database [31] and the National Institutes of Health Chest X-Ray Dataset [32], and from each dataset we randomly select 25 images to be used as the cover or secret. Since the resolutions of the images varies from around $512 \times 512$ to 4K, and we re-size them to $2048 \times 2048$ in the experiment for simplicity.

To the best of our knowledge, there is no similar approach that could offer equivalent capacity. Hence, we compare our method with a naive baseline model that modifies the Least Significant Bits (LSB) in the spatial domain (denoted as LSB). Concretely, we alter $1, 2$ bits of the carriers for hiding the RGB channels of the secret images. We employ the hyper-parameters $\lambda = 1.0$ and $\sigma = 0.05,\ 0.10$ for our method, which is named as SIC (Shuffled Image Concealing) in the table and figure. [3]

The experimental results are provided in Table 1. It can be seen that the LSB method suffers from a trade-off between the appearance of the observations and the reconstruction quality. Embedding with only 1 bit per color channel will severely degrade the quality of the secret images while embedding with 2 bits sharply hurts security, such that the embedded images can be easily observed by human beings. In the contrast, our proposed method provides the best reconstruction quality while keeps the appearances of observations at a reasonable level. Furthermore, it is worth mentioning that, the performance can be further improved by selecting hyper-parameters individually for each of the datasets, providing better flexibility in different situations than the LSB method. Examples of the results are provided in Figure 2.

### 3.2. Concealing images into audio signals

Besides using images as the cover carriers, in this subsection, we show an illustrative experiment to conceal image into the music waveform (The result is shown in Fig. 1). In contrast to the natural images, the single-channel music signals are generally formulated as high-dimensional vectors. However, we found that the music is significantly low rank if we reshaped it into a matrix. To support this claim, we evaluate the normalized singular values of several classical music fragments from the dataset "piano-midi". Specifically, we choose the music fragments from the musicians Chopin, Liszt, and Mozart. For each fragment, we only keep the first 1 million samples to generate the matrix ($1000 \times 1000$).

[2] https://www.gwern.net/Danbooru2017

[3] We also make an effort on implementing deep steganography for this task. Unfortunately, we could not train a network that could extract the RGB-color image from a signal gray-scale image after dozens of attempts.

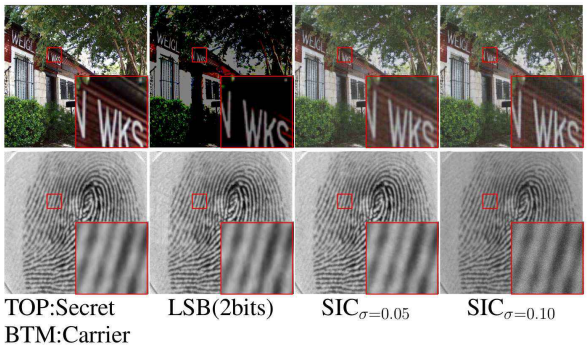


**Fig. 2**: Examples of concealing a grayscale or RGB color secret image into a grayscale carrier image.

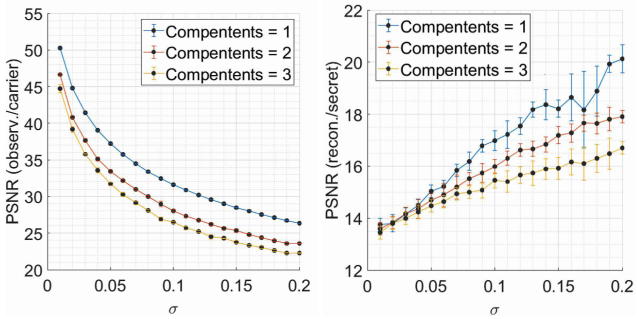


**Fig. 3**: The performance of the proposed method under different $\sigma$ configurations. In the figure, 1, 2 and 3 components are used as the secrets.

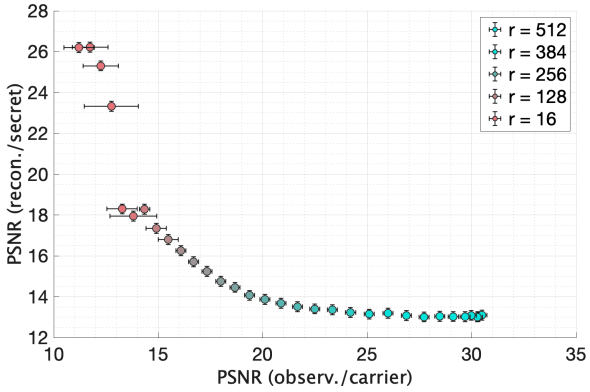


**Fig. 4**: The trade-off between the distinguishability of the observation and the quality of the reconstruction using $r$.

We observe that different musicians' music fragments have inherent low-rank structures that more than $80\%$ of the singular values are close to zero. The insight behind this characteristic is that the frequency of the music signals is mainly concentrated on a narrow frequency band. It implies that a small amount of Fourier bases can well approximate each piece of the signals. Hence, if we consider each column of the reshaped matrix as a piece of the music signal, then the columns will linearly dependent on each other when the size of the matrix is sufficiently large, *i.e.* the low-rank structure.

In the illustrative experiment, we employ our model to conceal the musician Chopin's full-size picture ($1000 \times 1000$ grayscale image. See Fig. 1 (a)) into the music signal. In the model, we configure the tuning parameters $\sigma = 0.005$ and $\lambda = 25$. We can see from Figure 1(b-c) that the carrier is just slightly distorted by the secret payload, but our model can still reconstruct the secret image with high precision. As aforementioned, the statistical characteristics of the payload are similar to AWGN due to the random shuffling operations. As shown in Fig. 1 (d), the power spectrum of the payload is about 50dB weaker than the carrier and has equal strength at different frequencies.

## 4. HYPER-PARAMETER SELECTION

### 4.1. Selection of $\sigma$

The $\sigma$ controls the strength of concealing, which balances between the distinguishability of the observation and the quality of the reconstruction. Concretely, a larger $\sigma$ for the secret image would make the observation looks more "noisy", while offering good quality of the reconstructed image. On the contrary, a smaller $\sigma$ for the secret image would cause less visual alteration in the carrier at the cost of the quality of the reconstructed image. Moreover, since the final image file will be quantized to integers within the range 0 to 255, the $\sigma$ could not be smaller than 1/255. Otherwise, all the embedded information will be lost during the quantization.

To illustrate this, we carry out several experiments using different $\sigma$ with different numbers of secrets. The changes of the PSNR in the observations and reconstructions are reported in Figure 3. The results show that the quality between the observation and the reconstruction can be balanced within a wide range.

### 4.2. Selection of the cover rank

Similar to $\sigma$, the truncated rank $r$ of the carrier also controls the trade-off between the distinguishability of the observation and the quality of the reconstruction. A smaller $r$ declines the visual details in the carrier while suppressing the interference of small singular values. To illustrate this, we further carry out experiments on synthesized datasets with controlled $r$ for carrier images. The results are given in Figure 4. We vary the $r$ of carrier images from 16 to 512 with stride 16, and fix the rank of secret images to be 64. We choice $\sigma = 0.1$ and $\lambda = 1.0$ for all the experiments.

## 5. DISCUSSION

In this paper, we propose a novel model for a lossy-style image concealing problem, in which we allow the acceptable reconstruction error on the secret images. Our model exploits the low-rank structure of the data to improve the payload capacity of concealing, which is completely different from the conventional bit-concealing-based methods. However, it is worth noting that there still exist several shortages in our model: (a) we don't consider the quantization error in our mathematical model, which may severely influence the reconstruction precision when we choose a small $\sigma$. (b) In the model, we indiscriminately modify every sample (pixel) of the cover carrier as the original LSB method, and this may make our concealing model more detectable. Hence, in future work, we consider only modify the samples (pixels) that are safe for attackers' detection. In this case, we need to alter our reconstruction methods to handle the incomplete components.

**Acknowledgement** The work is partially supported by JSPS KAKENHI (Grant No. 20K19875, 20H04249, 20H04208) and the National Natural Science Foundation of China (Grant No. 62006045).

## 6. REFERENCES


[1] Neil F Johnson and Sushil Jajodia, "Exploring steganography: Seeing the unseen," *Computer*, vol. 31, no. 2, pp. 26–34, 1998.

[2] Neil F Johnson and Sushil Jajodia, "Steganalysis of images created using current steganography software," in *International Workshop on Information Hiding*. Springer, 1998, pp. 273–289.

[3] Eckhard Koch and Jian Zhao, "Towards robust and hidden image copyright labeling," in *IEEE Workshop on Nonlinear Signal and Image Processing*. Neos Marmaras, Greece, 1995, vol. 1, pp. 123–132.

[4] Walter Bender, Daniel Gruhl, Norishige Morimoto, and Anthony Lu, "Techniques for data hiding," *IBM systems journal*, vol. 35, no. 3.4, pp. 313–336, 1996.

[5] Vojtěch Holub and Jessica Fridrich, "Designing steganographic distortion using directional filters," in *2012 IEEE International workshop on information forensics and security (WIFS)*. IEEE, 2012, pp. 234–239.

[6] Vojtěch Holub, Jessica Fridrich, and Tomáš Denemark, "Universal distortion function for steganography in an arbitrary domain," *Journal on Information Security*, vol. 2014, no. 1, pp. 1, 2014.

[7] Jarno Mielikainen, "LSB matching revisited," *IEEE signal processing letters*, vol. 13, no. 5, pp. 285–287, 2006.

[8] Tomáš Pevnỳ, Tomáš Filler, and Patrick Bas, "Using high-dimensional image models to perform highly undetectable steganography," in *International Workshop on Information Hiding*. Springer, 2010, pp. 161–177.

[9] Vahid Sedighi, Rémi Cogranne, and Jessica Fridrich, "Content-adaptive steganography by minimizing statistical detectability," *IEEE Transactions on Information Forensics and Security*, vol. 11, no. 2, pp. 221–234, 2016.

[10] Toby Sharp, "An implementation of key-based digital signal steganography," in *International Workshop on Information Hiding*. Springer, 2001, pp. 13–26.

[11] Della Baby, Jitha Thomas, Gisny Augustine, Elsa George, and Neenu Rosia Michael, "A novel DWT based image securing method using steganography," *Procedia Computer Science*, vol. 46, pp. 612–618, 2015.

[12] Po-Yueh Chen, Hung-Ju Lin, et al., "A DWT based approach for image steganography," *International Journal of Applied Science and Engineering*, vol. 4, no. 3, pp. 275–290, 2006.

[13] Vijay Kumar and Dinesh Kumar, "Performance evaluation of DWT based image steganography," in *Advance Computing Conference (IACC), 2010 IEEE 2nd International*. IEEE, 2010, pp. 223–228.

[14] Bassam J Mohd, Thaier Hayajneh, and Ahmad Nahar Quttoum, "Wavelet-transform steganography: Algorithm and hardware implementation," *International Journal of Electronic Security and Digital Forensics*, vol. 5, no. 3-4, pp. 241–256, 2013.

[15] Andreas Westfeld, "F5—a steganographic algorithm," in *International workshop on information hiding*. Springer, 2001, pp. 289–302.

[16] Shumeet Baluja, "Hiding images in plain sight: Deep steganography," in *Advances in Neural Information Processing Systems*, 2017, pp. 2069–2079.

[17] Clifford Bergman and Jennifer Davidson, "Unitary embedding for data hiding with the SVD," in *Security, Steganography, and Watermarking of Multimedia Contents VII*. International Society for Optics and Photonics, 2005, vol. 5681, pp. 619–631.

[18] Kuo-Liang Chung, Chao-Hui Shen, and Lung-Chun Chang, "A novel SVD-and VQ-based image hiding scheme," *Pattern Recognition Letters*, vol. 22, no. 9, pp. 1051–1058, 2001.

[19] Ryota Tomioka, Kohei Hayashi, and Hisashi Kashima, "On the extension of trace norm to tensors," in *NIPS Workshop on Tensors, Kernels, and Machine Learning*, 2010, p. 7.

[20] Ryota Tomioka and Taiji Suzuki, "Convex tensor decomposition via structured Schatten norm regularization," in *Advances in neural information processing systems*, 2013, pp. 1331–1339.

[21] Erik D Demaine and Martin L Demaine, "Jigsaw puzzles, edge matching, and polyomino packing: Connections and complexity," *Graphs and Combinatorics*, vol. 23, pp. 195–208, 2007.

[22] Emmanuel J Candès and Benjamin Recht, "Exact matrix completion via convex optimization," *Foundations of Computational mathematics*, vol. 9, no. 6, pp. 717, 2009.

[23] Emmanuel J Candès, Xiaodong Li, Yi Ma, and John Wright, "Robust principal component analysis?," *Journal of the ACM (JACM)*, vol. 58, no. 3, pp. 11, 2011.

[24] Ji Liu, Przemyslaw Musialski, Peter Wonka, and Jieping Ye, "Tensor completion for estimating missing values in visual data," *IEEE transactions on pattern analysis and machine intelligence*, vol. 35, no. 1, pp. 208–220, 2013.

[25] Jian-Feng Cai, Emmanuel J Candès, and Zuowei Shen, "A singular value thresholding algorithm for matrix completion," *SIAM Journal on Optimization*, vol. 20, no. 4, pp. 1956–1982, 2010.

[26] Chao Li, Mohammad Emtiyaz Khan, Zhun Sun, Gang Niu, Bo Han, Shengli Xie, and Qibin Zhao, "Beyond unfolding: Exact recovery of latent convex tensor decomposition under reshuffling," in *Proceedings of the AAAI Conference on Artificial Intelligence*, 2020, vol. 34, pp. 4602–4609.

[27] Edo Liberty, Franco Woolfe, Per-Gunnar Martinsson, Vladimir Rokhlin, and Mark Tygert, "Randomized algorithms for the low-rank approximation of matrices," *Proceedings of the National Academy of Sciences*, vol. 104, no. 51, pp. 20167–20172, 2007.

[28] M. Cimpoi, S. Maji, I. Kokkinos, S. Mohamed, and A. Vedaldi, "Describing textures in the wild," in *Proceedings of the IEEE Conf. on Computer Vision and Pattern Recognition*, 2014.

[29] Zhou Wang, Alan C Bovik, Hamid R Sheikh, and Eero P Simoncelli, "Image quality assessment: from error visibility to structural similarity," *IEEE transactions on image processing*, vol. 13, no. 4, pp. 600–612, 2004.

[30] Benjamin Weyrauch, Jennifer Huang, Bernd Heisele, and Volker Blanz, "Component-based face recognition with 3D morphable models," in *Proc. of CVPR Workshop on Face Processing in Video (FPIV'04), Washington DC, 2004*, 2004.

[31] Davide Maltoni, Dario Maio, Anil K Jain, and Salil Prabhakar, *Handbook of fingerprint recognition*, Springer Science & Business Media, 2009.

[32] Xiaosong Wang, Yifan Peng, Le Lu, Zhiyong Lu, Mohammadhadi Bagheri, and Ronald M Summers, "Chestx-ray8: Hospital-scale chest x-ray database and benchmarks on weakly-supervised classification and localization of common thorax diseases," in *Computer Vision and Pattern Recognition (CVPR), 2017 IEEE Conference on*. IEEE, 2017, pp. 3462–3471.